Impedance Properties of Electron Streams

By LISS C. PETERSON

The input impedance of an idealized space charge grid tube is investigated under general conditions of space charge between the accelerating grid and the negatively biased control grid. It is shown that under certain space charge conditions the input capacitance and conductance both may be negative. These impedance properties persist up to frequencies for which the transit angle is quite large. Possibilities of designing electronic negative capacitances are thus opened up. Experimental results are also given; these give a broad confirmation of the theoretical deductions.

PART I

Theory

IN the early stages of vacuum tube history the theoretical work on d-c. space charge treated mainly potential distributions associated with fairly small initial velocities of the electrons. With the advent of multi-electrode tubes this situation changed for it then became necessary to consider also potential distributions occurring when electrons are injected with large initial velocities. Idealizations were introduced to the extent that consideration was given only to space charge conditions which can exist between two parallel planes at known potentials when electrons with normal velocities corresponding to these potentials are injected into the region through one or both planes.[1]

Some time ago it was discovered experimentally that space charge may under certain conditions produce a negative capacitance. The negative capacitances were found during a series of low-frequency measurements of the control-grid-to-ground capacitance of an experimental space-charge-grid tube. In the course of these measurements it was found that with all the electrodes carefully by-passed to ground for a-c. except the negatively polarized control grid, the input capacitance as well as the input conductance was negative in certain domains which depended upon the d-c. operating voltages.

In order to arrive at an understanding of this fact, a-c. phenomena must be considered under the general d-c. space charge conditions

[1] Plato, Kleen, Rothe, *Zeitschrift f. Phys.*, *101*, July 1936. C. E. Fay, A. L. Samuel, W. Shockley, *Bell Sys. Tech. Jour.*, January 1938. B. Salzberg, A. V. Haeff, *R.C.A. Review*, January 1938.

referred to. The investigation comprises the calculation of the impedance between two parallel planes in vacuum, at known d-c. potentials, when an electron stream with normal d-c. velocities corresponding to these potentials is injected at right angles to the planes. As a further step, the effect of a negatively polarized grid interposed between the two planes will be considered. This latter arrangement may be taken to correspond to an idealized space charge grid tube.

Before these calculations are presented it is well to set forth as concisely as possible those results of the d-c. space charge analysis [1] which will be of most immediate interest. For this purpose we start with a qualitative review of the work of Fay, Samuel and Shockley.

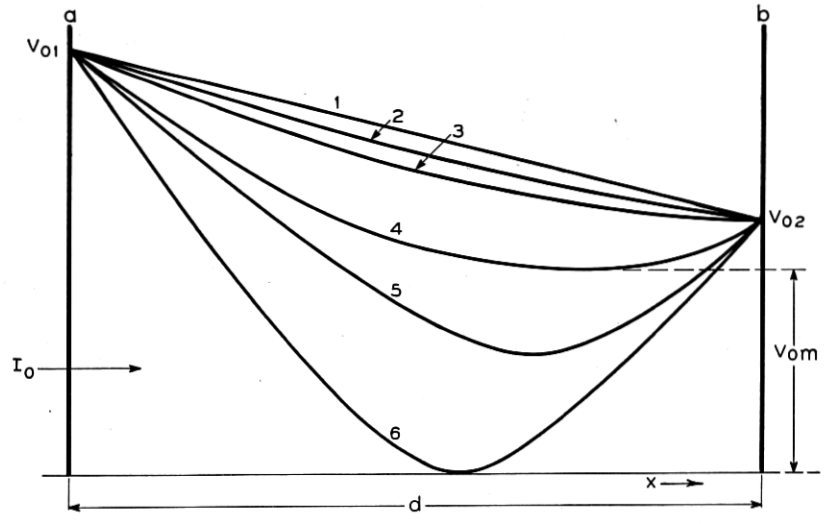

Fig. 1—Potential distributions between two planes of positive potential.

Consider two planes a and b, Fig. 1, of fixed d-c. potentials V_{01} and V_{02} ($V_{02} \leq V_{01}$) respectively, separated by a distance d. Let a unidirectional and uniform electron stream of I_0 amp./cm.^{2} be injected into the space from the left at right angles to the planes. When the injected current is extremely small the potential distribution does not differ very much from the free space one, represented by curve 1 on Fig. 1. As the injected current is increased slightly, the potential curve starts to sag, curve 2, and a further small increase causes a potential minimum to develop at the electrode of lower potential, curve 3. Still more increase in injected current makes the potential

[1] Loc. cit.

minimum V_{0m} sink and move towards the electrode of higher potential, curve 4. This state of affairs, with a continuously decreasing potential minimum, continues until a critical value of injected current is reached. The potential distribution may now be represented by curve 5. The slightest further increase in injected current causes the potential minimum to sink abruptly to zero: a virtual cathode is formed. This abrupt change will be referred to as a Kipp.

With this qualitative discussion of the various potential distributions in mind a more detailed classification may be made. If both planes are assumed to be at positive potentials we may classify the different potential distributions as follows:

1. Type B
2. Type C
3. Type D

Type B corresponds to virtual cathode operation. This mode of operation will be of no interest in this paper. Type C corresponds to the case when a potential minimum at positive potential is present between the planes and type D to the case when no such potential minimum is present. For the purpose of analysis it is convenient to distinguish between two types of D solution, i.e., D_1 and D_2. This comes about because the equations for potential distribution between the planes may exhibit a minimum outside the planes. The D_1 solutions correspond to the case when no such minimum exists and the D_2 solutions to the case when such a minimum does exist.

Let us consider Type C distributions in some more detail. For this purpose attention is directed to Fig. 2. Here the ratio $\frac{V_{0m}}{V_{01}}$ is shown as a function of the injected current I_0 with the ratio $\frac{V_{02}}{V_{01}}$ as parameter. The dotted curve represents a boundary line; for currents smaller than that given by this boundary no potential minimum can exist between the planes. Consider the curve $\alpha\beta\gamma$. At the point α the potential minimum sets in and as more current is injected the potential at the minimum decreases continuously until the point β is reached. Any further increase in current causes the potential minimum to sink abruptly to zero; thus β corresponds to the Kipp point. Now it is seen that within a section of the curve $\alpha\beta$ there are two possible solutions, namely those corresponding to the section $\beta\gamma_1$ of the upper branch and those corresponding to the lower branch $\beta\gamma$. Let us designate by C_1 space charge conditions corresponding to the upper branch $\alpha\beta$ and by C_2 those corresponding to the lower branch $\beta\gamma$.

After this survey of the several possible d-c. space charge conditions we may proceed to the a-c. phenomena involved. At the present time the impedance between the two planes of Fig. 1 can be found only if the electrons move in one direction, i.e. if no virtual cathode is present between the planes, and therefore this assumption is made. It will be further assumed that electrode "a" where the injection takes place is at a-c. ground potential. This insures constant conduction current and electron speed at the plane of injection. The impedance

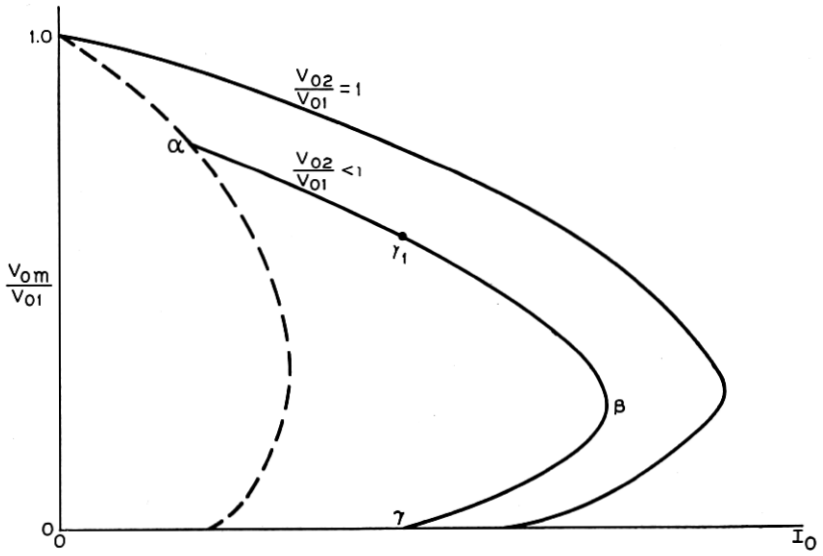

Fig. 2—Variations of the magnitude of the potential minimum as function of injected current.

may then be found by proper application of the general theory developed by Müller and Llewellyn.[2] The result is that the impedance may be represented by a series combination of a resistance r and a capacitance C having the values

$$r = J_0 \frac{T^4}{\epsilon} \cdot \frac{2 - 2\cos\theta - \theta\sin\theta}{\theta^4}$$

$$C = C_0 \cdot \frac{1}{1 - J_0 \frac{T^3}{d} \cdot \frac{2\sin\theta - \theta - \theta\cos\theta}{\theta^3}}, \qquad (1)$$

[2] J. Müller, *Hochfrequenztechnik u. Electroakustik*, May 1933; F. B. Llewellyn, *Bell Sys. Tech. Jour.*, October 1935.

where

$J_0 = \frac{e}{km\epsilon} I_0$

$\theta = \omega T$

$C_0 = \frac{\epsilon}{d}$ is the cold capacitance

T is transit time, seconds
e is electronic charge, coulombs
m is electronic mass, grams

$\frac{e}{m} = 1.77 \times 10^8$ coulomb/gm.

ϵ is permittivity of vacuum $= 8.85 \times 10^{-14}$ Farads/cm.[3]
$k = 10^{-7}$.

Present interest lies mainly in the range where the transit angle θ is small. Expanding (1) and assuming θ small, we have:

$$r = \frac{J_0 T^4}{12\epsilon}$$
$$C = C_0 \frac{1}{1 - J_0 \frac{T^3}{6d}}. \tag{2}$$

These formulas are also found in Müller's paper.[2]

With regard to the resistance r it is immediately seen that it is always positive and has the same equation as for complete space charge with current I_0 and transit time T.

From the capacitance equation it is immediately evident that an increase is caused by the presence of electrons. The dielectric constant of space charge under the stipulated conditions is seen to be dependent upon the d-c. conduction current I_0. As the injected current is increased the capacitance increases initially at a fairly slow rate, but as $J_0 \frac{T^3}{6d}$ becomes comparable with unity the capacitance rises rapidly. It becomes infinite for

$$J_0 \frac{T^3}{6d} = 1 \tag{3}$$

and if the left member of (3) were to become greater than unity the capacitance would be negative. The possibility of such a condition deserves careful consideration.

[2] Loc. cit.

From the discussion of the d-c. space charge it follows that the d-c. current has an upper limit; i.e., the Kipp current with the value

$$I_{0K} = \frac{4}{9}\epsilon\sqrt{\frac{2e}{mk}}\frac{(\sqrt{V_{01}} + \sqrt{V_{02}})^3}{d^2}. \tag{4}$$

To determine the relation between the Kipp current (4) and the current (3) required for infinite capacitance, consider the d-c. equations:

$$\begin{aligned} u_b &= u_a + a_a T + \frac{eI_0}{km\epsilon}\frac{T^2}{2} \\ d &= u_a T + a_a \frac{T^2}{2} + \frac{eI_0}{km\epsilon}\frac{T^3}{6}, \end{aligned} \tag{5}$$

where u_b and u_a are electron speeds in cm./sec. at planes b and a respectively and a_a is the acceleration in cm./sec.^{2} at plane a. Eliminating a_a and introducing the values of u_b and u_a in terms of V_{02} and V_{01} we find

$$T^3 - 6\sqrt{\frac{2m}{ek}}\frac{k\epsilon}{I_0}(\sqrt{V_{01}} + \sqrt{V_{02}})T + \frac{12km\epsilon}{I_0}d = 0. \tag{6}$$

When the transit time T is eliminated between (3) and (6) the result is

$$I_0 = \frac{4}{9}\epsilon\sqrt{\frac{2e}{mk}} \cdot \frac{(\sqrt{V_{01}} + \sqrt{V_{02}})^3}{d^2}. \tag{7}$$

But this is precisely the Kipp current as given by (4). Equation (3), therefore, expresses the Kipp relation between current and transit time. It has thus been found that the series capacitance at the Kipp point becomes infinite, whereas the impedance between the two planes is a pure resistance.

Consider next the possibility of $J_0\frac{T^3}{6d}$ attaining values larger than unity when the d-c. current I_0 is limited to values smaller than the Kipp value (4). The only manner in which this could happen would be for (6) to have one root T_2 such that $T_2 > T_k$ where T_k is the transit time at Kipp. To determine this (6) is transformed by introducing I_{0K} and T_K as parameters. Thus,

$$\left(\frac{T}{T_K}\right)^3\frac{I_0}{I_{0K}} - 3\frac{T}{T_K} + 2 = 0. \tag{8}$$

The discriminant D of (8) is

$$D = \left(\frac{I_{K0}}{I_0}\right)^2\left(1 - \frac{I_{K0}}{I_0}\right) \tag{9}$$

and as $I_0 \leq I_{K0}$ it is clear that

$$D \leq 0. \tag{10}$$

Hence, since the discriminant in general is negative (8) has three real roots. Two of these are positive and one negative. A double root occurs for $I_0 = I_{K0}$, and the value of this root is clearly $T = T_K$. For currents smaller than the Kipp current there are two positive roots T_1 and T_2 such that $T_1 < T_K$ and $T_2 > T_K$.

Thus it becomes evident that space charge conditions corresponding to the roots T_2 result in a negative capacitance. Interpreted in terms

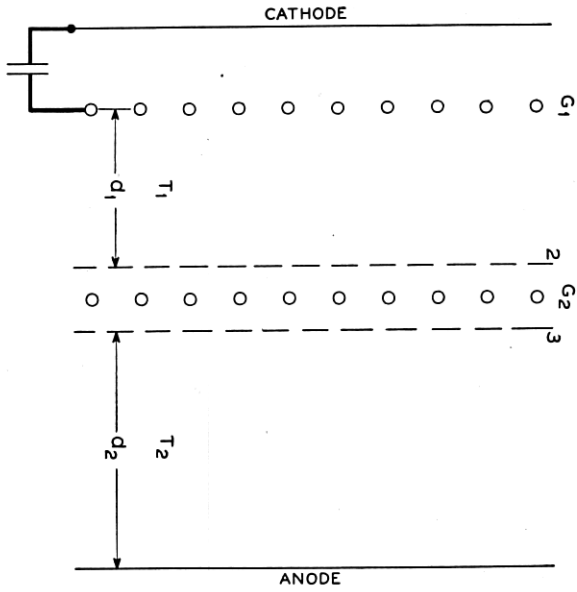

Fig. 3—Schematic of a space charge grid tube.

of Fig. 2, the roots T_1 correspond to the upper branch $\alpha\beta$ and the roots T_2 to the lower branch $\gamma\beta$. Hence, it is evident that space charge corresponding to the lower branch has a negative dielectric constant.

Consider next the system pictured schematically in Fig. 3. It differs basically from that in Fig. 1 in that a negatively polarized grid has been interposed between the planes a and b of Fig. 1. The arrangement shown in Fig. 3 may be considered to be equivalent to a space charge grid tube with the accelerating grid G_1 and control grid G_2. The grid G_1 is assumed to be by-passed to the cathode for a-c. The planes indicated by 2 and 3 are imaginary planes located

on opposite sides of the control grid wires and are assumed to be sufficiently far away from the grid to insure that the potential distribution at these planes is essentially that of a grid-free space. Moreover, if the grid is fine-meshed these planes may be located quite close together so that the distance between them is negligible in comparison with the distances between G_1 and plane 2, and between plane 3 and the plate. This insures that the potentials of the two planes are practically equal. Since the grid G_2 draws only displacement current, the conduction currents at the planes 2 and 3 are equal. Since the potentials of the two planes are equal, the electron speeds are also equal. The boundary conditions in the plane of G_1 are the same as those used in deriving (1), i.e., constant conduction current and electron-speed. Then, following the method employed by Llewellyn [2] in his treatment of the negative triode, the input impedance may be found. Since the details are uninteresting the result is merely quoted. On the assumption that the plate is short-circuited to the cathode by a large condenser the input impedance between grid and cathode may be written as:

$$Z = Z_g + \frac{A_1 A_2}{\epsilon(A_1 + A_2 + G_1 B_2 + D_1 C_2)}, \tag{11}$$

where Z_g is the impedance (capacitive) between the planes 2 or 3 and G_2 and where A_1, A_2, G_1, B_2, D_1 and C_2 have the values:

$$\left.\begin{aligned}
A_1 &= \frac{1}{(i\omega)^4}\left[(i\omega)^3 d_1 + \frac{eI_0}{km\epsilon}(2 - 2e^{-i\theta_1} - i\theta_1 - i\theta_1 e^{-i\theta_1})\right] \\
A_2 &= \frac{1}{(i\omega)^4}\left[(i\omega)^3 d_2 + \frac{eI_0}{km\epsilon}(2 - 2e^{-i\theta_2} - i\theta_2 - i\theta_2 e^{-i\theta_2})\right] \\
G_1 &= \frac{eI_0}{km\epsilon u_{02}(i\omega)^2}(1 - e^{-i\theta_1} - i\theta_1 e^{-i\theta_1}) \\
B_2 &= \frac{1}{(i\omega)^3}[a_{03}(i\theta_2 e^{-i\theta_2} + e^{-i\theta_2} - 1) + u_{02} i\omega(e^{-i\theta_2} - 1) \\
D_1 &= \frac{1}{(i\omega)^2}\left[1 - e^{-i\theta_1} - \frac{a_{02}}{i\omega u_{02}}(1 - e^{-i\theta_1} - i\theta_1 e^{-i\theta_1})\right] \\
C_2 &= \frac{eI_0}{km\epsilon(i\omega)^2}(i\theta_2 e^{-i\theta_2} + e^{-i\theta_2} - 1)
\end{aligned}\right\}. \tag{12}$$

In (12):

u_{02} is the d-c. speed at planes 2 or 3.

a_{02} and a_{03} are the d-c. accelerations at the planes 2 and 3 respectively.

[2] Loc. cit.

When the transit angles θ_1 and θ_2 are very small and when the effect of the space between control grid and anode may be ignored, evaluation of (11) yields the result:

$$Z = Z_g + r_1 \frac{1 - \frac{4}{3}\frac{J_0\frac{T_1^2}{2u_{02}}}{J_0\frac{T_1^3}{6d_1}} \cdot \frac{1 - J_0\frac{T_1^3}{6d_1}}{1 - J_0\frac{T_1^2}{2u_{02}}}}{1 - J_0\frac{T_1^2}{2u_{02}}} + \frac{1}{i\omega}\frac{1 - J_0\frac{T_1^3}{6d_1}}{C_0\left(1 - J_0\frac{T_1^2}{2u_{02}}\right)}, \quad (13)$$

where

$$\left.\begin{aligned} r_1 &= \frac{J_0}{\epsilon}\frac{T_1^4}{12} \\ C_0 &= \frac{\epsilon}{d_1} \end{aligned}\right\}. \quad (14)$$

C_0 is the capacitance in the absence of electrons.

The input impedance is thus seen to be a series circuit composed of a resistance and a capacitance, i.e.

$$Z = \rho + \frac{1}{i\omega C}, \quad (15)$$

where

$$\frac{1}{\rho} = \frac{1}{r_1} \cdot \frac{1 - J_0\frac{T_1^2}{2u_{02}}}{1 - \frac{4}{3}\frac{J_0\frac{T_1^2}{2u_{02}}}{J_0\frac{T_1^3}{6d_1}}\frac{1 - J_0\frac{T_1^3}{6d_1}}{J_0\frac{T_1^2}{2u_{02}}}}, \quad (16)$$

$$\frac{1}{C} = \frac{1}{C_g} + \frac{1}{C_0}\frac{1 - J_0\frac{T_1^3}{6d_1}}{1 - J_0\frac{T_1^2}{2u_{02}}}. \quad (17)$$

In studying the capacitance and resistance as functions of space charge it is evident from (16) and (17) that space charge enters essentially through the functions $\frac{J_0T_1^2}{2u_{02}}$ and $\frac{J_0T_1^3}{6d_1}$. In what follows

the capacitance C_g is assumed to be so large that the first term in (17) may be ignored. The ratio between "hot" and "cold" capacitance may then be written:

$$\frac{C}{C_0} = \frac{1 - J_0 \frac{T_1^2}{2u_{02}}}{1 - J_0 \frac{T_1^3}{6d_1}}. \tag{18}$$

Write the conductance $1/\rho$ as

$$\frac{1}{\rho} = \frac{1}{r_1} \cdot \mathrm{F} \tag{19}$$

and note that the first factor of the right member is always positive. F may be termed the relative input conductance.

Before the theoretical curves are discussed a few words about the functions $\frac{J_0 T_1^2}{2u_{02}}$ and $J_0 \frac{T_1^3}{6d_1}$ are in order. They will be expressed in terms of two parameters, i.e., φ and ξ where

$$\varphi = \frac{V_{02}}{V_{01}} \tag{20}$$

and ξ is a constant of integration which assumes different values depending upon the type of space charge present.[3] In terms of these parameters one may show that:

$$\left.\begin{aligned} J_0 \frac{T_1^3}{6d_1} &= \frac{[\sqrt{\xi^{1/2} + 1} - \sqrt{(\xi\varphi)^{1/2} + 1}]^3}{(\xi^{1/2} - 2)\sqrt{\xi^{1/2} + 1} - ((\xi\varphi)^{1/2} - 2)\sqrt{(\xi\varphi)^{1/2} + 1}} \\ J_0 \frac{T_1^2}{2u_{02}} &= \frac{[\sqrt{\xi^{1/2} + 1} - \sqrt{(\xi\varphi)^{1/2} + 1}]^2}{(\xi\varphi)^{1/2}} \end{aligned}\right\} \begin{array}{c}\text{Type} \\ D_1 \\ 0 < \xi < \infty,\end{array} \tag{21}$$

$$\left.\begin{aligned} J_0 \frac{T_1^3}{6d_1} &= \frac{[\sqrt{\xi^{1/2} - 1} - \sqrt{(\xi\varphi)^{1/2} - 1}]^3}{(\xi^{1/2} + 2)\sqrt{\xi^{1/2} - 1} - ((\xi\varphi)^{1/2} + 2)\sqrt{(\xi\varphi)^{1/2} - 1}} \\ J_0 \frac{T_1^2}{2u_{02}} &= \frac{[\sqrt{\xi^{1/2} - 1} - \sqrt{(\xi\varphi)^{1/2} - 1}]^2}{(\xi\varphi)^{1/2}} \end{aligned}\right\} \begin{array}{c}\text{Type} \\ D_2 \\ \frac{1}{\varphi} < \xi < \infty,\end{array} \tag{22}$$

[3] The parameters $1/\alpha$ and $1/\beta$ used by Fay, Samuel and Schockley are related to ξ as follows:

$$\xi = \frac{1}{\beta} \text{ Type } D_1$$

$$\xi = \frac{1}{\alpha} \text{ Type } D_2.$$

$$\left.\begin{aligned} J_0\frac{T_1^3}{6d_1} &= \frac{[\sqrt{\xi^{1/2}-1}+\sqrt{(\xi\varphi)^{1/2}-1}]^3}{(\xi^{1/2}+2)\sqrt{\xi^{1/2}-1}+((\xi\varphi)^{1/2}+2)\sqrt{(\xi\varphi)^{1/2}-1}} \\ J_0\frac{T_1^2}{2u_{02}} &= \frac{[\sqrt{\xi^{1/2}-1}+\sqrt{(\xi\varphi)^{1/2}-1}]^2}{(\xi\varphi)^{1/2}} \end{aligned}\right\} \text{Type } C_1 \quad \frac{1}{\varphi} < \xi < \left(1+\frac{1}{\sqrt{\varphi}}\right)^2. \tag{23}$$

The parameter ξ is without physical significance for the D solutions but serves merely as a convenient constant of integration. For the solutions of C type, however, ξ is of direct physical significance. For here ξ represents the ratio $\frac{V_{01}}{V_{0m}}$. In the language used in the previous qualitative discussion of space charge it is clear that $\xi = \frac{1}{\varphi}$ is the point where a potential minimum sets in and $\xi = \left(1+\frac{1}{\sqrt{\varphi}}\right)^2$ is the Kipp point. Calculations for C_2 solutions are not included.

The result of the calculations of capacitance and conductance are shown on Figs. 4 to 8. Figure 8 is an enlargement of Fig. 7 for small

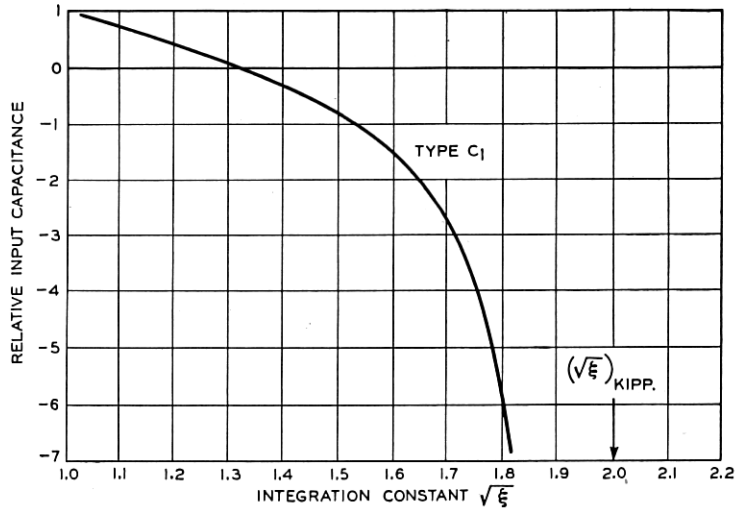

Fig. 4—Relative input capacitance of an idealized space charge grid tube for different space charge conditions (voltage ratio $\varphi = 1.0$).

values of F. Three values of the parameter φ were selected, i.e., 0.04, 0.25 and 1. The curves demonstrate regions of negative capacitance as well as of negative conductance. Note that as the parameter φ is made smaller both the capacitance and conductance pass through

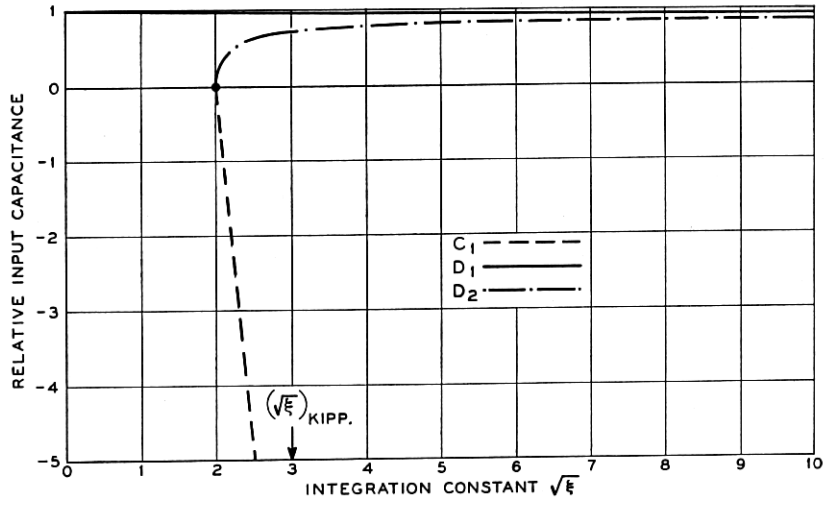

Fig 5—Relative input capacitance of an idealized space charge grid tube for different space charge conditions (voltage ratio $\varphi = 0.25$).

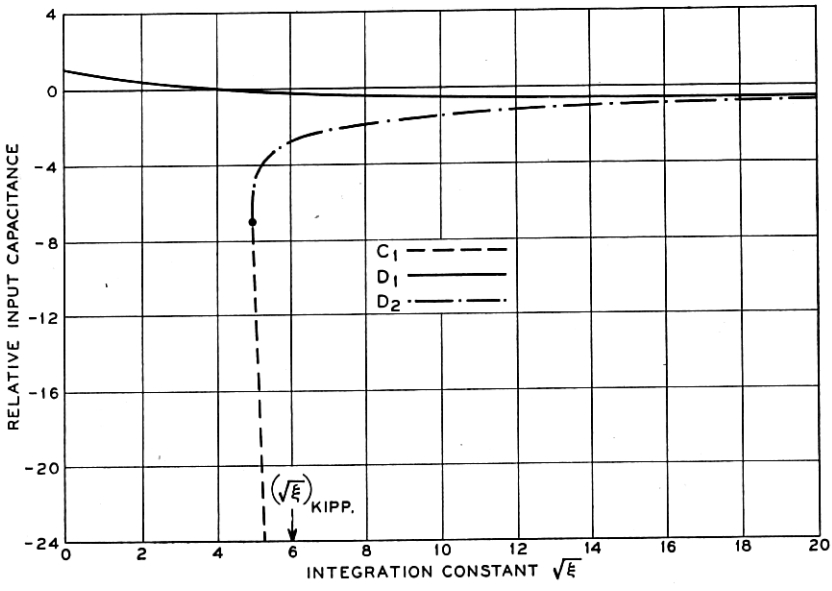

Fig. 6—Relative input capacitance of an idealized space charge grid tube for different space charge conditions (voltage ratio $\varphi = 0.04$).

zero for smaller values of ξ. Consider for instance the case for which $\varphi = 0.04$. The capacitance is here negative even in regions of small space charge and it is seen that over a wide range of the parameter ξ the capacitance is nearly constant. Both capacitance and conductance

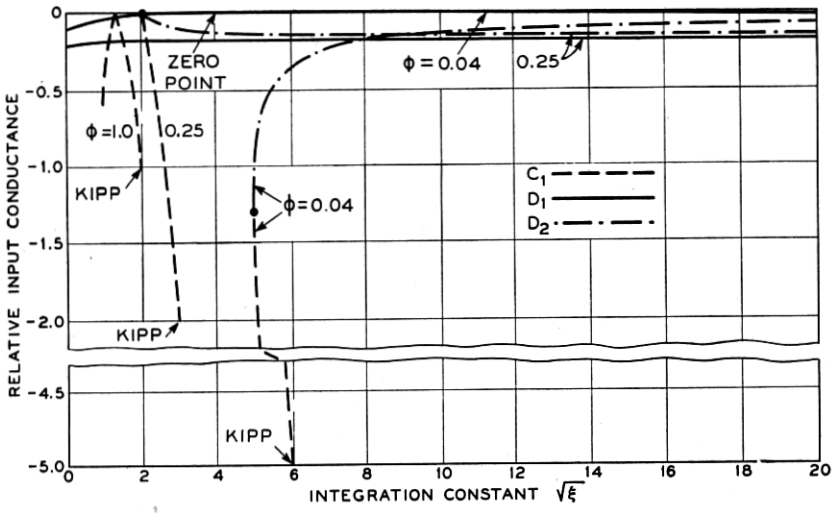

Fig. 7—Relative input conductance of an idealized space charge grid tube for different space charge conditions.

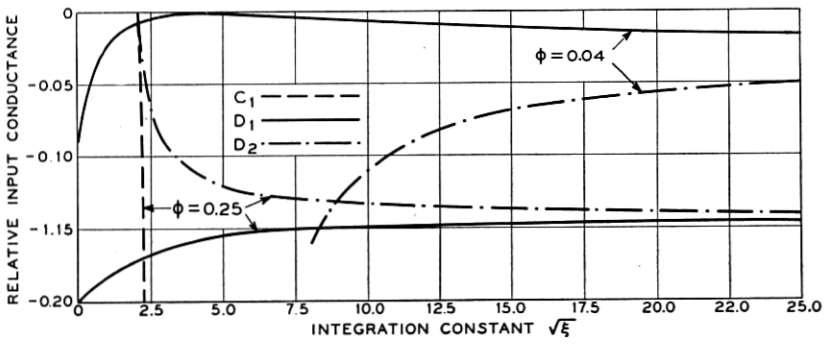

Fig. 8—Relative input conductance of an idealized space charge grid tube for different space charge conditions.

pass through zero for the same value of ξ and one sees that in case of $\varphi = 0.04$ no critical adjustment seems necessary. The conclusion is thus arrived at that the idealized space charge grid tube may be made to operate without input capacitance or loading up to moderately

high frequencies. In addition, the possibility of designing an electronic negative capacitance is opened up and this is a highly desirable objective.

However, it must be kept in mind that in the discussion, effects such as velocity distributions, electron deflections and dispersion forces have been neglected. Furthermore, in an actual tube the capacitance C_g must also be considered. At the Kipp the capacitance C is equal to $-\infty$; therefore, as the Kipp point is approached a positive capacitance is expected.

The capacitance and conductance both pass through zero when

$$J_0 \frac{T_1^2}{2u_{02}} = 1, \tag{24}$$

or when

$$u_{02} = J_0 \frac{T_1^2}{2}. \tag{25}$$

But in general

$$u_{02} = u_{01} + a_{01}T_1 + J_0 \frac{T_1^2}{2}, \tag{26}$$

where u_{01} and a_{01} are the d-c. speed and acceleration in the plane of grid G_1, Fig. 3.

The relation between initial speed and acceleration for zero capacitance and conductance is, therefore:

$$u_{01} + a_{01}T_1 = 0 \tag{27}$$

and since both u_{01} and T_1 are inherently positive, the initial acceleration must be negative. For the capacitance to be negative the requirement is obviously

$$u_{01} + a_{01}T_1 < 0. \tag{28}$$

Necessary requirements for a negative capacitance are thus a finite electron speed and a retarding field at the plane of injection.

PART II

Experimental

In this section some experimental results will be discussed. The measurements all refer to the capacitance between control grid and ground of some experimental tubes. The tubes were cylindrical in structure and contained two positive grids close to the cathode followed by a negative control grid. The first positive grid has the essential function of controlling the magnitude of the current whereas the

second determines the initial speed with which the electrons enter the space adjacent to the control grid.

In Fig. 9 the measured input capacitance and plate current are shown as functions of the voltage V_{g1} of the first grid. It is seen that as the plate current increases the capacitance gradually decreases, passes through zero somewhat before the plate current has reached its maximum and then becomes negative; it passes through a minimum and then gradually assumes a positive value equal to about twice the cold capacitance. This behavior of the capacitance is typical of the formation of a virtual cathode, which in the present instance appears

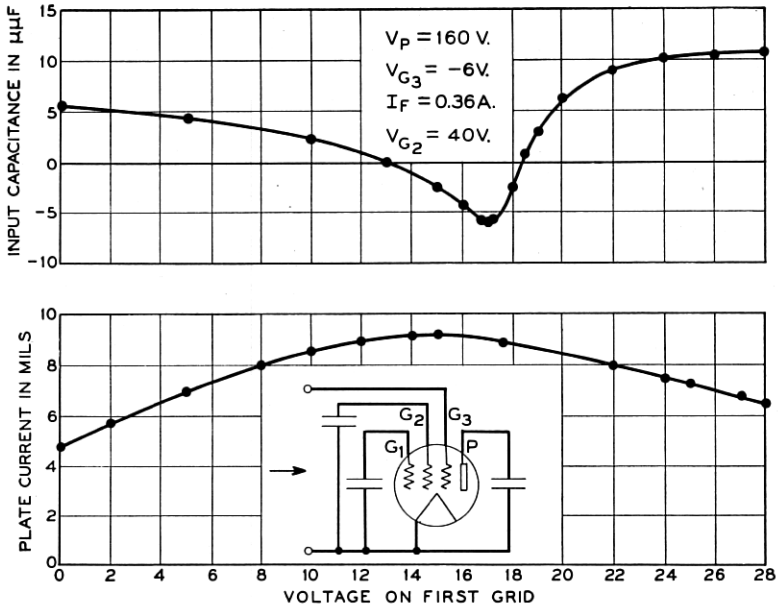

Fig. 9—Measured input capacitance of experimental vacuum tube no. 55 (grid signal = 0.18 volts r.m.s. at 50 kc.).

to be gradual. The negative capacitance is present in a small interval of the voltage V_{g1} immediately before and perhaps also during a part of the virtual cathode formation.

Figure 10 shows the measured input capacitance as a function of the control grid bias V_{g3} for several values of the voltage V_{g1}. For comparison purposes the corresponding plate currents are also shown. In the region of low plate current where a virtual cathode is present the capacitance is positive and larger than the cold capacitance. Where the plate current curve starts to bend over, that is, where the

virtual cathode starts to release, the capacitance decreases. It is negative in a small domain and turns ultimately positive. The plate current curve corresponding to $V_{g1} = 30$ volts indicates that the

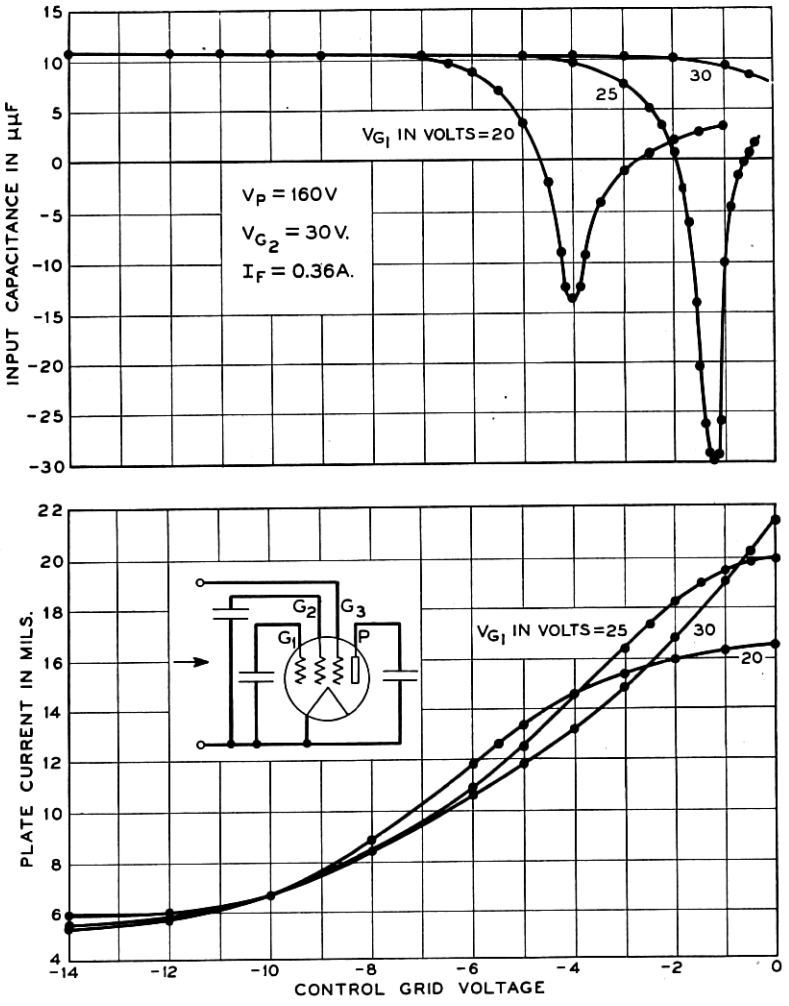

Fig. 10—Measured input capacitance of experimental vacuum tube no. 55 (grid signal = 0.18 volts r.m.s. at 50 kc.).

virtual cathode is present throughout the range of negative bias and the corresponding capacitance curve is positive everywhere.

Figure 11 refers to capacitance measurements on a tube in which a

Kipp occurred. Again the capacitance behaves essentially the same except that it suddenly jumps from a large negative value to the positive value corresponding to virtual cathode operation.

In comparing the theoretical and experimental results, it is seen that the theory gives predictions which are broadly in accord with experiments.

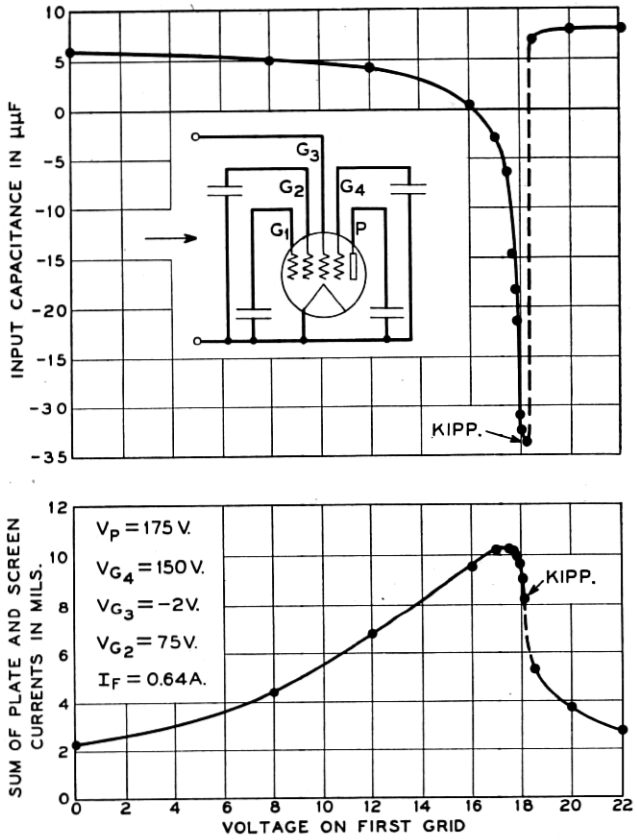

Fig. 11—Measured input capacitance of experimental vacuum tube no. 59 (grid signal = 0.05 volts r.m.s. at 50 kc.).

Acknowledgment

I am indebted to Mr. E. J. Buckley for assistance in the experimental work, to Miss M. Packer for the numerical calculations, to Mr. C. A. Bieling for the mechanical tube design, and last but not least to Dr. F. B. Llewellyn for stimulating discussions.